

Many-body systems as resources for universal fault tolerant quantum computation

Saubhik Sarkar,^{1,*} Chiranjib Mukhopadhyay,^{2,†} and Abolfazl Bayat^{3,‡}

¹*Institute of Physics, Polish Academy of Sciences, Aleja Lotnikow 32/46, PL-02668 Warsaw, Poland*

²*Quantum Information and Computation Group, Harish-Chandra Research Institute, HBNI, Allahabad 211019, India*

³*Institute of Fundamental and Frontier Sciences, University of Electronic Science and Technology of China, Chengdu 610051, China*

A universal quantum computer will inevitably rely on error correction to be fault tolerant. Most error correcting schemes are based on stabilizer circuits which fail to provide universal quantum computation. An extra quantum resource, in the form of magic states, is needed in conjunction with stabilizer circuits to perform universal quantum computation. However, creating, distilling, and preserving high quality magic states are not easy. Here, we show that quantum many-body systems are promising candidates to mine high quality magic states by considering transverse field anisotropic XY spin chains. In particular, we provide an analytic formula for the magic content of the qubits in the symmetry broken ground state of the XY spin chain, and show that there are two distinct scaling behaviors for magic near criticality. Moreover, we find an exact point in the phase diagram of the XY model at which every qubit of the system are pure H-states. This point represents a factorizable broken-symmetry ground state of the model. This is an excellent demonstration that many-body systems, even in the absence of ground state entanglement, are resourceful for fault tolerant universal quantum computation.

Introduction.— Quantum computers are believed to provide exponential advantage over their classical counterparts [1–3]. However, quantum systems are delicate, and inherently prone to error. Therefore, a genuine universal quantum computer must exhibit fault tolerance to be practically useful. Most fault tolerant schemes for quantum computation are based on stabilizer circuits, which not only fail to be universal, but can even be simulated efficiently by a classical computer [4]. Therefore, we need to augment stabilizer gates with other quantum resource states, known as *magic states*, to achieve universal fault tolerant quantum computation. The concept of magic [5] is operationally distinct from other well known quantum resources, nevertheless, the resource theory of magic [6–9] is intricately connected to entanglement [10, 11], coherence [12], and especially contextuality [13, 14], and non-Gaussianity [15–18]. Generating large numbers of quantum states with high degree of magic is challenging since magic is a fragile resource against external noise [12]. Hence, elaborate magic state distillation protocols have to be resorted to [5, 19–23], with limitations like existence of bound magic states [8, 24, 25]. One may thus legitimately raise the following question: is there any physical system that can naturally provide us with large quantity of reasonably high quality magic states with minimal tinkering?

Many-body systems provide a rich playground for different phases of matter [26, 27], mediating several tasks including quantum communication [28, 29], quantum metrology [30–33], remote gate implementation [34, 35], or refrigeration [36, 37]. Ground states of many-body systems are generically highly entangled at criticality [38, 39], and usually offer significant amounts of quantum resources, such as entanglement [27, 40–42] or quantum Fisher information [30, 31, 43]. Parallely, there exists points on the phase diagram of quantum many-body systems, for which the ground state is factorizable [44–46] into uncorrelated pure states, that may be reached from critical points via local operations and classical communication [47], and have been so far considered worth avoiding due to absence of entanglement. On the contrary, we

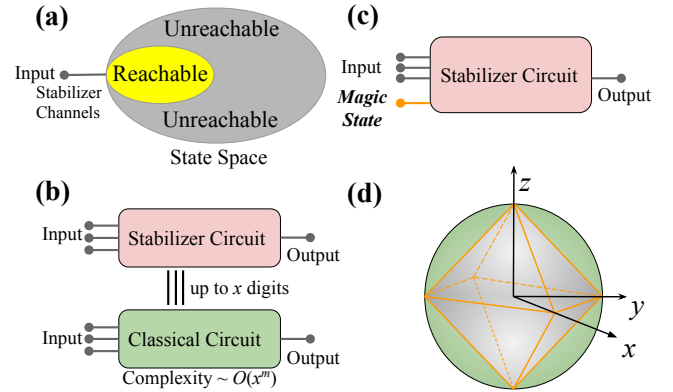


FIG. 1. **Schematics.** (a) Stabilizer codes allow access to a far smaller volume of the state space compared to an universal quantum computer (UQC). (b) Classical simulation of stabilizer circuits is efficient, i.e., can be performed with at most a polynomial overhead. (c) Paradigm of universal quantum computation through magic state injection. (d) Structure of the stabiliser hull (gray octahedron) inside the Bloch sphere.

show in this letter that these factorizable many-body ground states are excellent resources for obtaining a large number of highly magical pure H-states by considering a $U(1)$ -symmetry broken transverse field anisotropic XY spin chain. The ground state qubits lie within the stabilizer polytope throughout the disordered phase, and becomes *magical* immediately after the critical point. We demonstrate the existence of two different scaling behaviors in the vicinity of this point.

Magic state formalism.— A universal quantum computer is capable of implementing every unitary transformation on the Hilbert space of N qubits, where the size of the Hilbert space scales as 2^N . An important subset of unitary operators is the set of unitaries $\{U_{\text{stab}}\}$ that stabilize the Pauli operators under their action, such that $U_{\text{stab}}\sigma_i^\alpha U_{\text{stab}}^\dagger = \sigma_j^\beta$, where, σ_i^α denotes the α -th Pauli operator, with $\alpha \in \{0, x, y, z\}$ (the σ^0 stands for identity), acting on qubit i . These stabilizer unitaries are the

key ingredients for quantum error correction [48]. Although the stabilizer unitaries can generate entanglement [49], they are not capable of performing universal quantum computation in the sense that their action on a particular input bit string can only cover a subset of the entire Hilbert space, which is depicted in Fig. 1(a). In fact, the effect of a circuit comprising of stabilizer unitaries, see Fig. 1(b), is shown to be classically simulable in the sense that to achieve the precision of x -digits in the output, the depth of the minimally required (probabilistic) classical circuit scales polynomially with x [4]. This is in sharp contrast with a generic unitary operation, which can only be simulated by a classical circuit whose depth scales exponentially with x . Remarkably, the injection of some extra quantum resources, known as *magic* states, allows one to perform universal quantum computation, even with stabiliser circuits [5], which is schematically depicted in Fig. 1(c). Note that, magic is distinct from other quantum mechanical resources, e.g., entanglement. For instance, product states, or even single qudit states, can be magic states, while certain highly entangled states, e.g., cluster states, contain no magic [49]. In this context, the *free*, i.e., non-magical states, are called *stabilizer* states, which are states generated from the action of stabilizer unitaries on a bit string $|0, 0, \dots, 0\rangle$, and any convex mixture. In the case of single qubits, the stabilizer unitaries are the Pauli operators together with the Hadamard and the phase gates [6], whose actions on $|0\rangle$ generate six pure stabilizer states. Therefore, the stabilizer states are inside the octahedron inscribed within the Bloch sphere, as shown in Fig. 1(d) [6, 50], and quantum states outside the octahedron represent magic states. For multiqubit systems, entanglement generating gates such as CNOTs have to be also added to the set of stabilizer unitaries.

Quantification of magic.— There are different approaches for quantification of magic. In this letter, we use the *Robustness of Magic* (RoM) [7, 9, 50] for an arbitrary quantum state ρ , which is defined as

$$R(\rho) := \inf_{S_k \in S} \left\{ m \geq 0 : \frac{\rho + mS_k}{1+m} \in S \right\}, \quad (1)$$

where S is the set of stabilizer states. The RoM $R(\rho)$ quantifies the the minimum contribution of stabilizer states needed to be mixed with the quantum state ρ to make it stabilizer too. To simplify the computation of $R(\rho)$, one can use the overcompleteness of the stabilizer states and write the density matrix ρ as a pseudomixture of stabilizer states $S_k \in S$ such that $\rho = \sum_k X_k S_k$, where the weights $\{X_k\}$ are in general, arbitrary real numbers satisfying the normalization constraint $\sum_k X_k = 1$. If ρ is a stabilizer state, then it is possible to find at least one such decomposition where all $\{X_k\}$ s are positive. However, if ρ is not a stabilizer state, at least one of the weights X_k is negative. In Ref. [8], it has been shown that the RoM can be alternatively expressed as

$$R(\rho) = \min_{\{X_k\}} \left\{ \sum_k |X_k| - 1 : \rho = \sum_k X_k S_k, S_k \in S \right\}.$$

This minimization problem can be linearized to,

$$R(\rho) = \min_{\{X_k\}} \left\{ \sum_k |X_k| - 1 : AX = B \right\}, \quad (2)$$

where $A_{\alpha\beta} = \text{Tr}(\sigma^\alpha S_\beta)$ and $B_\alpha = \text{Tr}(\sigma^\alpha \rho)$, with σ^α as the α -th Pauli operator. For example, in the qubit case, A is a 4×6 matrix and B is a 4×1 vector. This can be cast in the form of a linear programming problem, and can be solved numerically via any convex optimization package. In particular, it is worth emphasizing that the maximum magic for a single qubit confined to one of the equatorial planes of the Bloch sphere, quantified by RoM, is $\sqrt{2} - 1$, which is achieved for the H -qubit states [9, 50].

Model.— We consider a chain of N interacting qubits with the transverse field anisotropic XY Hamiltonian [51, 52],

$$H = -J \sum_{i=1}^{N-1} \left(\frac{1+\gamma}{2} \sigma_i^x \sigma_{i+1}^x + \frac{1-\gamma}{2} \sigma_i^y \sigma_{i+1}^y \right) - h \sum_{i=1}^N \sigma_i^z, \quad (3)$$

where J is the exchange coupling, γ is the anisotropy parameter, and h is the magnetic field strength. As $\lambda = J/h$ varies, this system exhibits a second order quantum phase transition in its ground state from an ordered to a disordered phase with the critical point located at $\lambda = \lambda_c = 1$. The $U(1)$ -symmetry broken ground state of this model is factorizable iff $\lambda = 1/\sqrt{1-\gamma^2}$ [46]. The attractiveness of this model lies in the fact that it can be solved analytically, even in the thermodynamic limit ($N \rightarrow \infty$) [53, 54]. The quantum phase transition can be captured by the longitudinal magnetization $\langle \sigma^x \rangle$ as the order parameter of the model, which is nonzero in the ordered ferromagnetic phase for $\lambda > 1$, and vanishes in the disordered paramagnetic phase. It may be noted that the condition $\gamma = 1$ corresponds to the usual transverse Ising model, and the condition $\gamma = 0$ corresponds to the isotropic XY chain. The reduced density matrix of any qubit at site i is written as $\rho_i = \frac{1}{2} \sum_{\alpha=0,x,y,z} \langle \sigma_i^\alpha \rangle \sigma_i^\alpha$, where $\langle \sigma_i^\alpha \rangle$ is the average of the corresponding Pauli operator σ_i^α with respect to the ground state. For this model, $\langle \sigma_i^y \rangle$ vanishes for all values of λ and γ , allowing us to write (see supplementary material [55]), the single qubit RoM in the following simple form

$$R_\gamma(\lambda) = \max [\langle \sigma^x \rangle + \langle \sigma^z \rangle - 1, 0]. \quad (4)$$

This is the first result of this letter and we drop the index i since the system is translationally invariant. In the thermodynamic limit, the longitudinal magnetization $\langle \sigma^x \rangle$, as the order parameter of the system, has a compact analytic form [54]

$$\langle \sigma^x \rangle = \sqrt{\frac{2}{1+\gamma}} \left[\gamma^2 (\lambda_c^{-2} - \lambda^{-2}) \right]^{\beta_x} g(\lambda), \quad (5)$$

where $g(\lambda) = 1$ in the ordered phase, and vanishes in the disordered phase (see, e.g., Ref. [39] for detailed discussions), and $\beta_x = \frac{1}{8}$. The transverse magnetization $\langle \sigma_z \rangle$ is given in

terms of elliptical integrals [54], which have to be computed numerically, in the following way in the thermodynamic limit

$$\langle \sigma^z \rangle = \frac{1}{\pi} \int_0^\pi \frac{1 + \lambda \cos \phi}{\sqrt{(\gamma \lambda \sin \phi)^2 + (1 + \lambda \cos \phi)^2}} d\phi. \quad (6)$$

In the extreme regime of the paramagnetic phase, i.e., $\lambda \rightarrow 0$, all the spins point towards the magnetic field, and show no magic. Deep in the ordered phase $\lambda \rightarrow \infty$, the ground state takes a GHZ form $\frac{1}{\sqrt{2}}(|0, 0, \dots, 0\rangle - |1, 1, \dots, 1\rangle)$ [39], and thus every single qubit is maximally mixed, and hence non-magical. Near the critical point however, the ground state is highly entangled, and thus one may wonder whether any magic would emerge in the quantum state of the system.

Magic at the vicinity of the critical point.— When λ is close to the critical point λ_c in the ordered phase, the order parameter $\langle \sigma^x \rangle$, given by Eq. (5), scales approximately as $\langle \sigma^x \rangle = K_x (\lambda - \lambda_c)^{\beta_x}$, where K_x is a constant, expressible in terms of the anisotropy parameter γ [39]. The derivative of the transverse magnetization has a logarithmic divergence near criticality, but $\langle \sigma^z \rangle$ also can be numerically approximated by the algebraic behavior, $\langle \sigma^z \rangle \simeq \langle \sigma^z \rangle_c + K_z (\lambda - \lambda_c)^{\beta_z}$, where $\langle \sigma^z \rangle_c$ is the transverse magnetization at the critical point, and β_z, K_z are γ -dependent constants. It is noteworthy that $\beta_z \gg \beta_x$ for all possible values of $\gamma \in (0, 1]$ [55].

For every anisotropy parameter γ , one can locate a value of $\lambda = \lambda_c^*(\gamma)$, such that the RoM vanishes for every $\lambda \leq \lambda_c^*$, and finite thereafter. We call this point $\lambda_c^*(\gamma)$ as the *magic pseudocritical point* (MPP). Although $\lambda_c^*(\gamma)$ is very close to the critical point, it always lies in the ordered phase. Note that the existence of an MPP is a consequence of the definition of RoM in Eq. (4), and does not imply a new criticality. Nonetheless, we call λ_c^* the MPP, since the amount of magic $R_\gamma(\lambda)$ exhibits power law scaling behavior in the vicinity of λ_c^* , as shown below. We first rewrite Eq. (4), by inserting the algebraic behaviors of $\langle \sigma_x \rangle$ and $\langle \sigma_z \rangle$, and by using the constraint $R_\gamma(\lambda_c^*) = 0$, as

$$R_\gamma(\lambda) = K_x \left((\lambda - \lambda_c)^{\beta_x} - \delta \lambda_c^{\beta_x} \right) + K_z \left((\lambda - \lambda_c)^{\beta_z} - \delta \lambda_c^{\beta_z} \right), \quad (7)$$

where $\delta \lambda_c = \lambda_c^* - \lambda_c$ is the distance between the MPP and the critical point. The above result is valid for $\lambda > \lambda_c^*$. When the parameter λ is in very close vicinity of the MPP, determined by $\lambda - \lambda_c^* \ll \delta \lambda_c$, keeping terms up to first order in $(\lambda - \lambda_c^*)/\delta \lambda_c$ in the expression of RoM in Eq. (7) results in the following linear scaling behavior about the MPP

$$R_\gamma(\lambda) = T_\gamma (\lambda - \lambda_c^*), \quad \text{for } \lambda - \lambda_c^* \ll \delta \lambda_c, \quad (8)$$

where the prefactor is given by $T_\gamma = K_x \beta_x (\delta \lambda_c)^{\beta_x - 1} + K_z \beta_z (\delta \lambda_c)^{\beta_z - 1}$. Beyond this regime, when $\lambda - \lambda_c^* > \delta \lambda_c$, the RoM has contributions from two algebraic behaviors, as given in Eq. (7), up to a constant which depends on the anisotropy parameter γ . As β_x is smaller than β_z the dominant behavior of the RoM stems from the first term in Eq. (7), i.e., $R_\gamma(\lambda) \simeq K_x (\lambda - \lambda_c)^{\beta_x} + \text{const}$. Hence, the derivative of RoM scales as

$$\frac{\partial R_\gamma(\lambda)}{\partial \lambda} \propto (\lambda - \lambda_c)^{\beta_x - 1}. \quad (9)$$

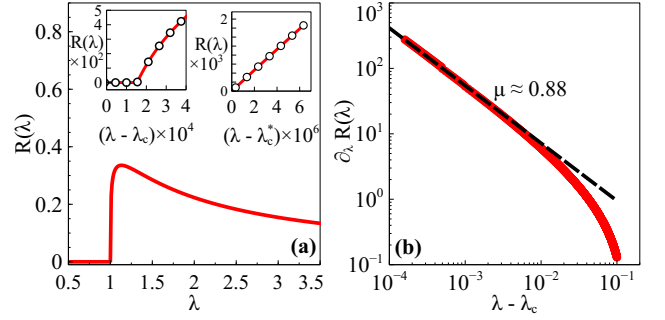


FIG. 2. **Infinite transverse Ising chain.** (a) RoM for the ground state of infinite transverse Ising chain plotted vs. λ . *Left inset:* magic rises at the MPP which is slightly after λ_c . *Right inset:* linear scaling of RoM near the MPP. (b) The derivative of RoM plotted against deviation from criticality in a log-log plot.

We note that this expansion is about the critical point, and as such, valid for all $\lambda > \lambda_c^*$ reasonably near criticality. Demonstration of these two different scaling behaviors, given in Eqs. (8) and (9), is the second result of this letter.

Results for transverse Ising chain.— We first focus on the special case of the transverse Ising chain ($\gamma=1$) in the thermodynamic limit. Using the analytic form of $\langle \sigma^z \rangle$ from Eq. (5) and numerically computing $\langle \sigma^z \rangle$ from Eq. (6) one can compute $R_{\gamma=1}(\lambda)$ using Eq. (4). In Fig. 2(a), we plot the RoM $R_{\gamma=1}(\lambda)$ as a function of the control parameter λ . As the left inset of Fig. 2(a) shows, the rising of magic from zero, namely MPP, is very close to the critical point, and takes place at around $\lambda_c^* = 1.00015$. After the MPP, the magic rises very steeply and reaches its maximum around $\lambda = \lambda_{\max} = 1.1313$, and then decays slowly as λ increases further. Since the MPP is very close to the critical point, the region for linear scaling of magic, as given by Eq. (8), is very small, and captured in the right inset of Fig. 2(a). In Fig. 2(b), we plot the derivative $\partial_\lambda R_{\gamma=1}(\lambda)$ as a function of $\lambda - \lambda_c$ in the log-log scale, which shows algebraic behavior of the form $\partial_\lambda R_{\gamma=1}(\lambda) \sim (\lambda - \lambda_c)^{-\mu}$, with $\mu = 0.88$. The fitting parameter μ is very close to $1 - \beta_x$ (with $\beta_x = 1/8$) giving an excellent agreement with the prediction of Eq. (9).

Results for anisotropic XY chain.— We now consider the more general case of the anisotropic XY chain, where $\gamma < 1$. In Fig. 3(a), we plot $R_\gamma(\lambda)$ as a function of both anisotropy parameter γ and the control parameter λ . Again, for a fixed value of γ , as λ varies, there is a sharp rise in the magic right after the MPP until it reaches its maximum $R_\gamma^{\max} = R_\gamma(\lambda = \lambda_{\max})$, and then decays gradually. In Fig. 3(b), we plot the MPP as a function of γ . As the figure shows, λ_c^* remains very close to λ_c , and monotonously moves towards $\lambda_c = 1$, as the anisotropy in the Hamiltonian decreases. Interestingly, the deviation $\delta \lambda_c$ shows power law scaling with γ , i.e., $\delta \lambda_c \sim \gamma^{5.55}$. Approaching the isotropic limit as $\gamma \rightarrow 0$, magic in the system vanishes for any value of the control parameter λ , as the longitudinal magnetization $\langle \sigma^x \rangle$ vanishes throughout. The corresponding scaling exponents μ is plotted for various anisotropy parameters γ in Fig. 3(c) which shows small variations near $1 - \beta_x$. The rea-

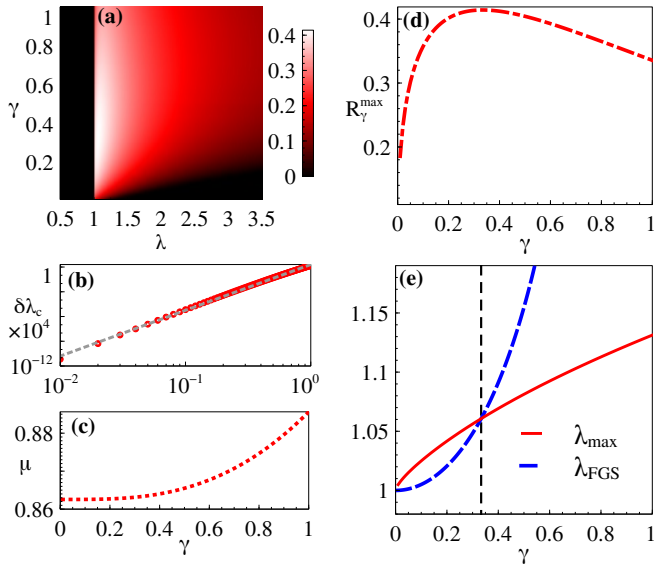


FIG. 3. **Infinite transverse XY chain.** (a) Density plot of RoM at ground state as a function of λ and γ . (b) Deviation of the MPP λ_c^* from actual critical point λ_c for different anisotropy parameters (red circles), which shows a scaling behavior with exponent ≈ 5.55 (gray dashed fitting line). (c) Critical exponent μ calculated for different γ 's. (d) Maximum RoM attainable in single qubit symmetry-broken ground states vs. γ . (e) The parameter values of λ at maximal RoM, λ_{\max} (red solid line), and at the point where ground state is factorized, λ_{FGS} (blue dashed line) intersect exactly where the global maxima of RoM is reached (black broken line).

son that μ slightly varies across the phase diagram is due to sub-dominant corrections from $\langle \sigma^z \rangle$. In Fig. 3(d), we plot the maximum magic R_γ^{\max} as a function of anisotropy parameter γ . Interestingly, the R_γ^{\max} peaks at $\gamma = 0.3333$, with the corresponding $\lambda_{\max} = 1.0606$, and reaches its maximum value of $\sqrt{2} - 1$ (up to the set accuracy of numerical evaluation), which is the maximum attainable magic from a qubit confined to an equatorial plane of the Bloch sphere [9, 50]. In Fig. 3(e), we show that the globally optimal magic in the parameter space (λ, γ) , is created when the ground state is factorized [44–46]. This is a particularly remarkable result, since the factorized single-qubit ground state is pure, the ground state for this parameter value is demonstrably a pure H -state. Finding this point in the phase diagram at which a large number of H -state qubits are obtainable and its correspondence with the factorization point is our third and main result of this letter.

Finite size scaling.— In practice, all systems are finite and, therefore, it would be more relevant to study magic in such systems. However, analytic results are difficult to obtain for finite chains as: (i) the assumption of translational invariance breaks down; (ii) the approach of finding the magnetization $\langle \sigma^x \rangle$ from the corresponding two site correlation functions fails. We use numerical methods based on density matrix renormalization group based algorithm [56–58] with matrix product states and matrix product operator techniques [59, 60], with bond dimension 300, and magnitude of symmetry-breaking field $\sim 10^{-8} h$. For computational pur-

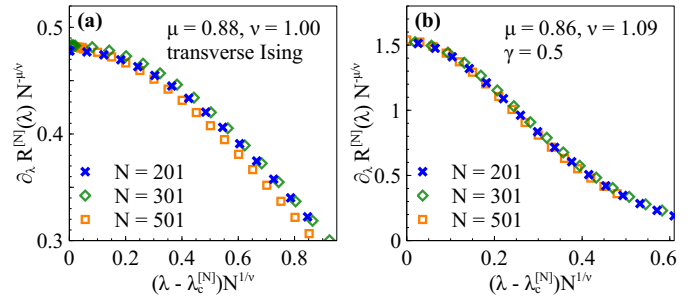


FIG. 4. **Finite size scaling.** Finite size scaling of the transverse XY chain for : (a) $\gamma = 1$, i.e., transverse Ising chain, and (b) $\gamma = 0.5$.

poses, we consider the central site to minimize the boundary effects. To be specific, we perform the finite size scaling analysis to extract the critical exponents, some of which have been directly calculated in the previous sections. Inspired by Eq. (9), we suggest a finite size ansatz [61] for the the derivative of magic as

$$\partial_\lambda R_\gamma^{[N]}(\lambda) \sim N^{\mu/\nu} f\left(N^{1/\nu}(\lambda - \lambda_c^{[N]})\right), \quad (10)$$

where $f(\cdot)$ is an arbitrary function and $\lambda_c^{[N]}$ is the finite size critical point at which the derivative of the order parameter $\langle \sigma^x \rangle$ peaks. In Figs. 4(a)-(b), we plot $\partial_\lambda R_\gamma^{[N]}(\lambda)N^{-\mu/\nu}$ as a function of $N^{1/\nu}(\lambda - \lambda_c^{[N]})$ for various system sizes for the transverse Ising case and for $\gamma = 0.5$, respectively. By tuning μ and ν , we collapse the curves corresponding to such systems. The best collapse is achieved with $\mu=0.88$, $\nu=1.00$ for the transverse Ising case, and with $\mu=0.86$, $\nu=1.09$ for the case when $\gamma=0.5$. In both cases, the exponents are quite close to the value of the scaling exponent μ extracted from the infinite chain behavior, as demonstrated in Fig. 3(c). Thus, the finite size scaling behavior is consistent with the infinite chain case considered earlier.

Conclusion.— In this letter, we have shown that many-body systems can be considered as resources for fault tolerant universal quantum computation as they provide us with high quality magic states in the ordered phase of the anisotropic XY model. We have three main results in this letter: (i) an analytic compact formula for single qubit magic in the ground state of the XY model; (ii) discriminating two different scaling behaviors at the vicinity of the critical point; and most importantly, (iii) specifying an exact point in the phase diagram, coinciding with the factorization point, in which the system provides almost perfect magic states, demonstrating the power of many-body systems in providing high quality magic states for fault tolerant universal quantum computation. Moreover, we have performed finite size scaling analysis to numerically show how the thermodynamic features can be extracted from finite-sized systems.

Acknowledgements.— Discussions with Anton Buyskhikh and Sougato Bose are warmly acknowledged. SS acknowledges the support of the (Polish) National Science Center Grant No. 2016/22/E/ST2/00555. CM acknowledges doc-

toral fellowship from the Department of Atomic Energy, Government of India, as well as funding from INFOSYS. CM thanks University College London and the UESTC in China for their kind hospitality. AB acknowledges the National Key R&D Program of China, Grant No. 2018YFA0306703. The computational works were performed using the Interdisciplinary Centre for Mathematical and Computational Modelling, University of Warsaw (ICM), under Computational Grant No. G75-6.

* sarkar@ifpan.edu.pl

† chiranjibmukhopadhyay@hri.res.in

‡ abolfazl.bayat@uestc.edu.cn

- [1] P. Shor, *SIAM Journal on Computing* **26**, 1484 (1997).
- [2] M. Araújo, F. Costa, and Č. Brukner, *Phys. Rev. Lett.* **113**, 250402 (2014).
- [3] M. Gu, K. Wiesner, E. Rieper, and V. Vedral, *Nature Communications* **3**, 762 (2012).
- [4] D. Gottesman, arXiv:quant-ph/9807006 (1998).
- [5] S. Bravyi and A. Kitaev, *Phys. Rev. A* **71**, 022316 (2005).
- [6] V. Veitch, S. A. Hamed Mousavian, D. Gottesman, and J. Emerson, *New Journal of Physics* **16**, 013009 (2014).
- [7] M. Ahmadi, H. B. Dang, G. Gour, and B. C. Sanders, *Phys. Rev. A* **97**, 062332 (2018).
- [8] E. T. Campbell and D. E. Browne, *Phys. Rev. Lett.* **104**, 030503 (2010).
- [9] M. Howard and E. Campbell, *Phys. Rev. Lett.* **118**, 090501 (2017).
- [10] G. Tóth and O. Gühne, *Phys. Rev. A* **72**, 022340 (2005).
- [11] K. M. R. Audenaert and M. B. Plenio, *New Journal of Physics* **7**, 170 (2005).
- [12] C. Mukhopadhyay, S. Sazim, and A. K. Pati, *Journal of Physics A: Mathematical and Theoretical* **51**, 414006 (2018).
- [13] X. Zhan, X. Zhang, J. Li, Y. Zhang, B. C. Sanders, and P. Xue, *Phys. Rev. Lett.* **116**, 090401 (2016).
- [14] M. Howard, J. Wallman, V. Veitch, and J. Emerson, *Nature* **510**, 351 (2014).
- [15] F. Albarelli, M. G. Genoni, M. G. A. Paris, and A. Ferraro, *Phys. Rev. A* **98**, 052350 (2018).
- [16] R. Takagi and Q. Zhuang, *Phys. Rev. A* **97**, 062337 (2018).
- [17] V. Veitch, C. Ferrie, D. Gross, and J. Emerson, *New Journal of Physics* **14**, 113011 (2012).
- [18] A. Mari and J. Eisert, *Phys. Rev. Lett.* **109**, 230503 (2012).
- [19] C. Jones, *Phys. Rev. A* **87**, 042305 (2013).
- [20] W. Zheng, Y. Yu, J. Pan, J. Zhang, J. Li, Z. Li, D. Suter, X. Zhou, X. Peng, and J. Du, *Phys. Rev. A* **91**, 022314 (2015).
- [21] E. T. Campbell, H. Anwar, and D. E. Browne, *Phys. Rev. X* **2**, 041021 (2012).
- [22] J. O’Gorman and E. T. Campbell, *Phys. Rev. A* **95**, 032338 (2017).
- [23] E. T. Campbell and M. Howard, *Phys. Rev. A* **95**, 022316 (2017).
- [24] E. T. Campbell, *Phys. Rev. A* **83**, 032317 (2011).
- [25] H. Dawkins and M. Howard, *Phys. Rev. Lett.* **115**, 030501 (2015).
- [26] S. Sachdev, *Handbook of Magnetism and Advanced Magnetic Materials* (2007).
- [27] L. Amico, R. Fazio, A. Osterloh, and V. Vedral, *Rev. Mod. Phys.* **80**, 517 (2008).
- [28] S. Bose, *Phys. Rev. Lett.* **91**, 207901 (2003).
- [29] S. Bose, *Contemp. Phys.* **48**, 13 (2007).
- [30] P. Zanardi, M. G. Paris, and L. C. Venuti, *Phys. Rev. A* **78**, 042105 (2008).
- [31] C. Invernizzi, M. Korbman, L. C. Venuti, and M. G. Paris, *Phys. Rev. A* **78**, 042106 (2008).
- [32] I. Frérot and T. Roscilde, *Phys. Rev. Lett.* **121**, 020402 (2018).
- [33] C. L. Degen, F. Reinhard, and P. Cappellaro, *Rev. Mod. Phys.* **89**, 035002 (2017).
- [34] N. Y. Yao, L. Jiang, A. V. Gorshkov, Z.-X. Gong, A. Zhai, L.-M. Duan, and M. D. Lukin, *Phys. Rev. Lett.* **106**, 040505 (2011).
- [35] L. Banchi, A. Bayat, P. Verrucchi, and S. Bose, *Phys. Rev. Lett.* **106**, 140501 (2011).
- [36] L. A. Correa, J. P. Palao, G. Adesso, and D. Alonso, *Phys. Rev. E* **87**, 042131 (2013).
- [37] M. H. Mohammady, H. Choi, M. E. Trusheim, A. Bayat, D. Englund, and Y. Omar, *Phys. Rev. A* **97**, 042124 (2018).
- [38] O. F. G. Osterloh, A. and R. Fazio, *Nature* **416**, 608 (2002).
- [39] T. J. Osborne and M. A. Nielsen, *Phys. Rev. A* **66**, 032110 (2002).
- [40] G. Vidal, J. I. Latorre, E. Rico, and A. Kitaev, *Phys. Rev. Lett.* **90**, 227902 (2003).
- [41] A. Bayat, S. Bose, P. Sodano, and H. Johannesson, *Phys. Rev. Lett.* **109**, 066403 (2012).
- [42] A. Bayat, *Phys. Rev. Lett.* **118**, 036102 (2017).
- [43] Z. Sun, J. Ma, X.-M. Lu, and X. Wang, *Phys. Rev. A* **82**, 022306 (2010).
- [44] S. M. Giampaolo, G. Adesso, and F. Illuminati, *Phys. Rev. Lett.* **100**, 197201 (2008).
- [45] S. M. Giampaolo, G. Adesso, and F. Illuminati, *Phys. Rev. B* **79**, 224434 (2009).
- [46] B. Tomasello, D. Rossini, A. Hamma, and L. Amico, *EPL (Europhysics Letters)* **96**, 27002 (2011).
- [47] J. Cui, M. Gu, L. C. Kwok, M. F. Santos, H. Fan, and V. Vedral, *Nature Communications* **3**, 812 (2012).
- [48] D. Lidar and T. Brun, *Quantum Error Correction* (Cambridge University Press, 2013).
- [49] H. J. Briegel, “Cluster states,” in *Compendium of Quantum Physics*, edited by D. Greenberger, K. Hentschel, and F. Weierert (Springer Berlin Heidelberg, Berlin, Heidelberg, 2009) pp. 96–105.
- [50] M. Heinrich and D. Gross, arXiv:1807.10296 (2018).
- [51] E. Lieb, T. Schultz, and D. Mattis, *Annals of Physics* **16**, 407 (1961).
- [52] A. Dutta, G. Aeppli, B. K. Chakrabarti, U. Divakaran, T. F. Rosenbaum, and D. Sen, *Quantum Phase Transitions in Transverse Field Spin Models: From Statistical Physics to Quantum Information* (Cambridge University Press, 2015).
- [53] E. Barouch, B. M. McCoy, and M. Dresden, *Phys. Rev. A* **2**, 1075 (1970).
- [54] E. Barouch and B. M. McCoy, *Phys. Rev. A* **3**, 786 (1971).
- [55] (See supplementary material).
- [56] G. Vidal, *Phys. Rev. Lett.* **93**, 040502 (2004).
- [57] A. J. Daley, C. Kollath, U. Schollwöck, and G. Vidal, *J. Stat. Mech.* **2004**, P04005 (2004).
- [58] S. R. White and A. E. Feiguin, *Phys. Rev. Lett.* **93**, 076401 (2004).
- [59] F. Verstraete, V. Murg, and J. Cirac, *Adv. Phys.* **57**, 143 (2008).
- [60] U. Schollwöck, *Ann. Phys. January 2011 Special Issue*, **326**, 96 (2011).
- [61] M. Barber, *Finite size scaling*, *Phase Transitions and critical phenomena*, edited by C. Domb and J.L. Leibovitz, Vol. 8 (Academic Press, London, 1983) pp. 146–259.

SUPPLEMENTARY MATERIAL

A. Simpler formula for RoM relevant to our purpose

In the spin chain model considered in the letter, the reduced density matrix has zero magnetization along the y -axis, i.e., $\langle \sigma^y \rangle = 0$. Any such qubit state ρ can be expressed as the (possibly non-convex) sum of four stabiliser states. We assume thst, the optimal decomposition, in the context of calculating the RoM, is of the following form

$$\rho = a_1|0\rangle\langle 0| + a_2|1\rangle\langle 1| + a_3|+\rangle\langle +| + a_4|-\rangle\langle -|. \quad (\text{S1})$$

The expectation values are $\langle \sigma^x \rangle = a_3 - a_4$, and $\langle \sigma^z \rangle = a_1 - a_2$, which are both positive. Now, If all of the a_i 's are non-negative, the state is within the stabiliser polytope. On the other hand, these quantities can not all be negative because of the positive semi-definiteness of density matrix. This leaves us with three different alternatives.

1. *If three of the coefficients are negative* – We assume without loss of generality that a_2, a_3, a_4 is negative while a_1 is positive. Combining this with the normalization condition $a_1 + a_2 + a_3 + a_4 = 1$ means that a_1 must be greater than 1. Therefore, $\langle \sigma^z \rangle = a_1 - a_2$ is greater than one, which is a contradiction. Thus, this case does not arise.

2. *If only one coefficient is negative* – Without loss of generality, let us assume only a_4 is negative. In this case, we adopt the strategy of showing that there for every such decomposition, either the state is a stabilizer state or there always exists another decomposition with two negative coefficients which leads to a lower RoM - hence this choice can not be an optimal decomposition. To this end, let us first choose a $\mu \in (0, 1)$ such that $a_2 + \mu a_4 = -\epsilon$, where ϵ is an arbitrarily small positive real number. If no such μ can be found in this range, then choose a $\mu \geq 1$ for which $a_2 + \mu a_4 = 0$. Thus, since $a_1 > a_2$, it is always possible to choose ϵ in such a way that $a_1 + \mu a_4$ is a positive number. Now, let us note that $|0\rangle\langle 0| + |1\rangle\langle 1| = |+\rangle\langle +| + |-\rangle\langle -|$, substituting this in the assumed optimal decomposition yields the following decomposition for ρ , $\rho = (a_1 + \mu a_4)|0\rangle\langle 0| + (a_2 + \mu a_4)|1\rangle\langle 1| + (a_3 - \mu a_4)|+\rangle\langle +| + (1 - \mu)a_4|-\rangle\langle -|$.

Now, let us note that only the coefficients of $|1\rangle\langle 1|$, and $|-\rangle\langle -|$ may be negative here. If $\mu < 1$, then the new decomposition with two negative coefficients leads to a lower RoM value of $2|1 - \mu| + 2\epsilon$, which is less than the assumed optimal decomposition if ϵ is arbitrarily small. If $\mu \geq 1$, then the state lies within the stabilizer polytope

since all the coefficients are now positive. Hence the proof is complete.

3. *If two of the coefficients are negative* – Without loss of generality, we assume a_1 , and a_3 are both positive, while a_2 , and a_4 are both negative. Hence, the RoM is given by $-2a_2 - 2a_4 = (a_1 - a_2) - (a_1 + a_2) + (a_3 - a_4) - (a_3 + a_4) = \langle \sigma^z \rangle + \langle \sigma^x \rangle - 1$.

Thus, the formula in the main text (Eq. (4)), that RoM equals $\max[0, \langle \sigma^x \rangle + \langle \sigma^z \rangle - 1]$, is proved.

B. Scaling of transverse magnetisation

In this subsection, we present numerical evidence that the transverse magnetization has an algebraic behavior near criticality, i.e.,

$$\langle \sigma^z \rangle \simeq \langle \sigma^z \rangle_c + K_z(\lambda - \lambda_c)^{\beta_z}. \quad (\text{S2})$$

As is depicted in Fig. S1, the algebraic behavior of transverse magnetization close to the critical point is clear. The scaling exponent β_z broadly lies in the range $\in (0.8, 0.9)$. The detailed values of scaling exponents β_z for different values of anisotropy are reported in the following table. The fitting lines are shown in the corresponding figure.

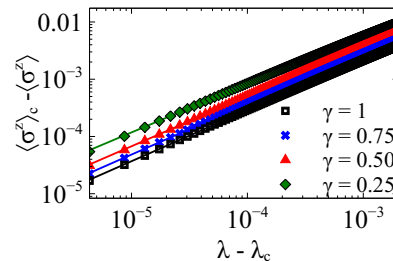


FIG. S1. Scaling of deviation of transverse magnetization $\langle \sigma^z \rangle$ from its magnitude at λ_c , with deviation from criticality $\lambda - \lambda_c$ for an infinite transverse XY chain with different γ (points), and corresponding linear fits (solid straight line.).

Anisotropy γ	Exponent β_z
0.25	0.8545
0.5	0.8780
0.75	0.8888
1.00	0.8919

TABLE S1. Exponent β_z for different anisotropy parameters γ corresponding to Fig. S1 above.